NAVAL SHIP RESEARCH AND DEVELOPMENT CENTER

Bethesda, Maryland 20084



COMPARATIVE SEAKEEPING CHARACTERISTICS OF TWO UNITED STATES COAST GUARD PATROL BOATS IN REGULAR WAVES

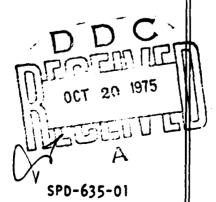
by

N. K. Bales

APPROVED FOR PUBLIC RELEASE: DISTRIBUTION UNLIMITED

SHIP PERFORMANCE DEPARTMENT

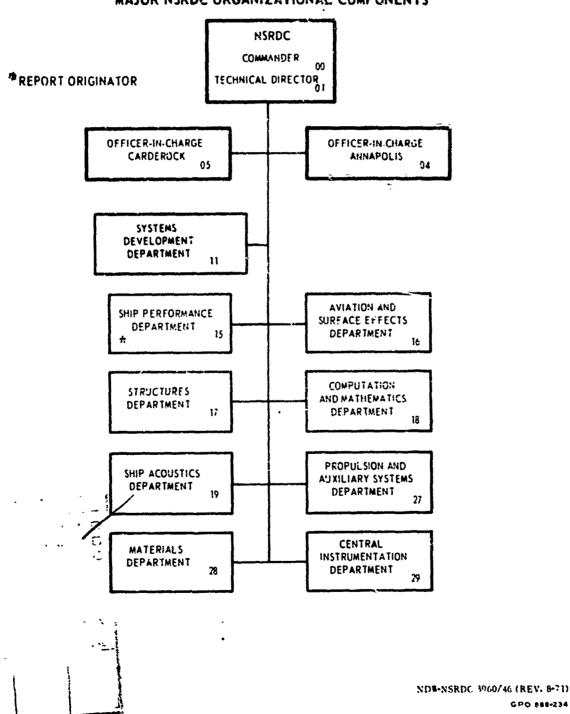
September 1975



The Navat Ship Research and Development Center is a U. S. Navy center for laboratory effort directed at achieving improved sea and air vehicles. It was formed in March 1967 57 merging the David Taylor Model Basin at Carderock, Maryland with the Marine Engineering Laboratory at Annapolis, Maryland

Naval Ship Research and Development Center Bethesda, Md. 20034

MAJOR NSRDC ORGANIZATIONAL COMPONENTS



GPO 888-234

UNCLASSIFIED
SECURITY CLASSIFICATION OF THIS PAGE 1 THE Date Entered)

REPORT DOCUMENTATION PAGE	READ INSTRUCTIONS BEFORE COMPLETING FORM
	3 RESIPIENT' SATALOG NUMBEN
SPD-635-01)	
A STATE OF THE STA	S. TYPE OF REPORT & PERIOD COVE
COMPARATIVE SEAKEEPING CHARACTERISTICS OF TWO UNITED STATES COAST GUARD PATROL BOATS IN	Final repting
REGULAR WAVES	. PERFORMING ORG REPORT NUMBE
1-2-10-10-	8 CONTRACT OR GRANT NUMBER(s)
N. K. dales	
PERFORMING ORGANIZATION NAME AND ADDRESS	10 PROGRAM ELEMENT PROJECT TA
David W. Taylor Naval Ship R&D Center	AREA & WORK UNIT NUMBERS
Bethesda, Maryland 20084	Work Unit 1=1568-013
11 CONTROLLING OFFICE NAME AND ADDRESS	7 /10
United States Coast Guard 400 Seventh Street, S.W.	13 NUMBER OF PAGES
Washington D.C. 20590 14 MONITORING AGENCY NAME & ADDRESSIII dillorar from Controlling Office)	18 SECURITY CLASS (of this report)
	UNCLASSIFIED
	194 DECLASSIFICATION DOWNGRADIN
16 DISTRIBUTION STATEMENT (of this Report)	<u> </u>
APPROVED FOR PUBLIC RELEASE: DISTRIBUTION UNLI	MITED
APPROVED FOR PUBLIC RELEASE: DISTRIBUTION UNL!	
17 DISTRIBUTION STATEMENT (c) the ebetract antered in Block 30, if different fo	
17 DISTRIBUTION STATEMENT (c) the ebetract entered in Block 20, if different for the estimate of the estimate	om Report;
17 DISTRIBUTION STATEMENT (c) the ebatract entered in Black 30, if different for supplement ARY NOTES. 18 SUPPLEMENTARY NOTES.	om Report;
17 DISTRIBUTION STATEMENT (c) the ebetract entered in Block 20, if different for the estimate of the estimate	om Report;
17 DISTRIBUTION STATEMENT (c) the obstract entered in Block (2), if different for supplies the supplies of the	em Report)
17 DISTRIBUTION STATEMENT (c) the obstract entered in Black 20, if different for SUPPLEMEN"ARY NOTES 18 SUPPLEMEN"ARY NOTES 19 KEY WORDS (Continue on reverse side if necessary and identify by black number Seakeeping, Pairol Boats, Effect of Hull Form 20 Austract (Continue on reverse side if necessary and identify by black number)	om Report)
17 DISTRIBUTION STATEMENT (c) the observed entered in Black 20, if different for the supplementary notes 18 SUPPLEMENTARY NOTES 19 KEY WORDS (Continue on reverse side if necessary and identify by block number Seakeeping, Pairol Boats, Effect of Hull Form 20 Austract (Continue on reverse side if necessary and identify by block number). The seakeeping characteristics of two, Unit boats (a 95-foot WPB and a 140-foot WAGB) are cobased on computed, nondimensional, responses in	ted States Coast Guard patrompared. The comparison is regular waves. On this
DISTRIBUTION STATEMENT (ci the obstract entered in Black 20, if different for SUPPLEMEN ARY NOTES 18 SUPPLEMEN ARY NOTES 19 KEY WORDS (Continue on reverse elde if necessary and identify by block number Seakeeping, Pairol Boats, Effect of Hull Form 20 Austract (Continue on reverse elde if necessary and identify by block number, The seakeeping characteristics of two, Unit boats (a 95-foot WPB and a 140-foot WAGB) are coloated on computed, nondimensional, responses in basis, the seakeeping characteristics of the 95-	ted States Coast Guard patrompared. The comparison is regular waves. On this
17 DISTRIBUTION STATEMENT (c) the observed entered in Black 20, if different for the supplementary notes 18 SUPPLEMENTARY NOTES 19 KEY WORDS (Continue on reverse side if necessary and identify by block number Seakeeping, Pairol Boats, Effect of Hull Form 20 Austract (Continue on reverse side if necessary and identify by block number). The seakeeping characteristics of two, Unit boats (a 95-foot WPB and a 140-foot WAGB) are cobased on computed, nondimensional, responses in	ted States Coast Guard patrompared. The comparison is regular waves. On this

DD 1 JAN 79 1473

289 674 -

UNCLASSIFIED

SECURITY CLASSIFICATION OF THIS PAGE (When Does Enter

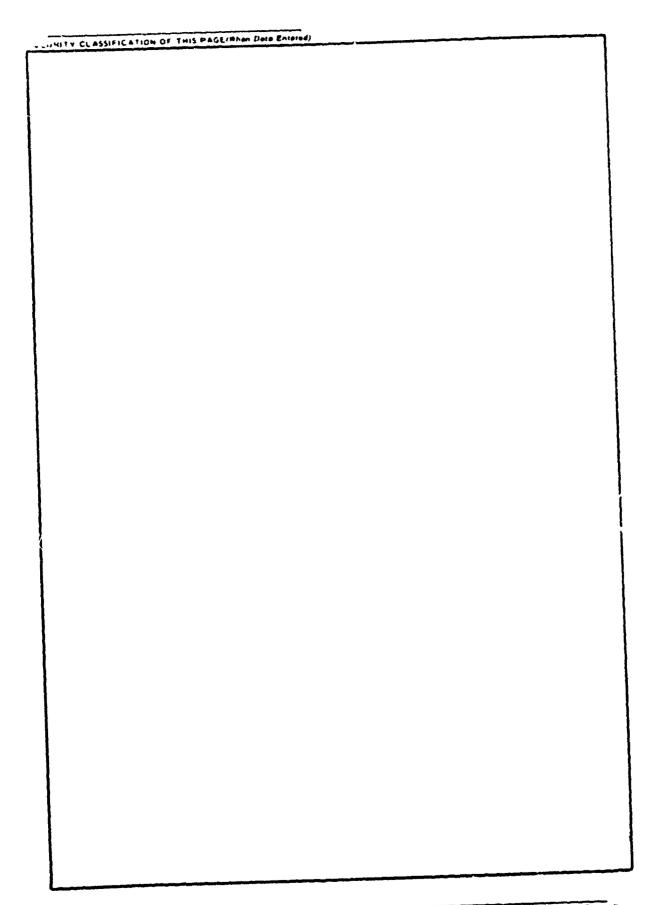


TABLE OF CONTENTS

ABSTRACT	Page 1
ADMINISTRATIVE INFORMATION	1
INTRODUCTION	1
DATA BASE COMPUTATIONS	1
MALYSIS	3
CONCLUSION	5
ACKNOWLEDGMENTS	5
REFERENCES	6
Table 1 - Properties of the 95-Foot WPB and of the 140-Foot WAGB LIST OF FIGURES	7
Figure 1 - Computer Representation of 95-Foot WPB Hull	8
Figure 2 - Computer Representation of 140-Foot WAGB Hull	9
Figure 3 - Roll Maxima at $F_n = 0.10 \dots \dots \dots \dots$	10
Figure 4 - Roll Maxima at $F_n = 0.27 \dots \dots \dots \dots$	11
Figure 5 - Roll Maxima at $F_n = 0.44 \dots \dots \dots \dots$	12
Figure 6 - Pitch Maxima at $F_n = 0.10 \dots \dots \dots \dots$	13
Figure 7 - Pitch Maxima at $F_n = 0.27 \dots \dots \dots \dots$	14
Figure 8 - Fitch Maxima at $F_n = 0.44 \dots$	15
Figure 9 - Heave Maxima at $F_n = 0.10 \dots \dots \dots \dots$	

Figure	10	-	Heave Maxima at $F_n = 0.\overline{2}7$	Page 17
Figure	11	-	Heave Maxima at $F_n = 0.44$	18
Figure	12	-	Acceleration Maxima at $F_n = 0.10 \dots \dots$	19
Figure	13	-	Acceleration Maxima at $F_n = 0.27 \dots \dots \dots$	20
Figure	14	-	Acceleration Maxima at $F_n = 0.44 \dots \dots \dots \dots$	21
Figure	15	-	Roll Transfer Functions at μ = 90 Degrees and F_n = 0.10	22
Figure	16	-	Roll Transfer Functions at $\mu = 120$ Degrees and $F_n = 0.44$	23
Figure	17	-	Pitch Transfer Functions at μ = 150 Degrees and F_n = 0.44	24
Figure	18	-	Heave Transfer Functions at μ = 180 Degrees and F_n = 0.44	25
Figure	19	-	Acceleration Transfer Functions at μ = 180 Degrees and F = 0.44	26
Figure	20	-	Cosine of Heave-to-Pitch Phase Angles at μ = 150 Degrees and F_n = 0.10	27

NOTATION

B _x	Maximum beam on load waterline
Fn	Froude number
L _{BP}	Ship length between perpendiculars
^T ₩	Draft amidships
GM	Metacentric height
KB	Vertical distance from center of buoyancy to keel
LCB	Longitudinal center of buoyancy
LCF	Lo gitudinal center of flotation
ZG	Vertical distance from load waterline to center of gravity
9	Acceleration of gravity
k ₉	Radius of gyration in pitch
k _o	Radius of gyration in roll
» _A	Single amplitude of absolute vertical acceleration
z _A	Single amplitude of heave
Δ	Ship displacement
μ	Heading of ship relative to waves
εzθ	Heave-to-pitch phase angle
ζA	Single amplitude of wave
θA	Single amplitude of pitch
v _H	Maximum wave slope
ф _А	Single amplitude of roll
λ/L	Ratio of wavelength to ship's length between perpendiculars

ABSTRACT

The seakeeping characteristics of two, United States Coast Guard patrol boats (a 95-foot WPB and a 140-foot WAGB) are compared. The comparison is based on computed, nondimensional, responses in regular waves. On this basis, the seakeeping characteristics of the 95-foot boat are found to be superior to those of the 140-foot boat.

ADMINISTRATIVE INFORMATION

The work reported herein was funded by the United States Coast Guard under Military Interdepartmental Purchase Request Z-70099-4-44131, and was identified at the David W. Taylor Naval Ship Research and Development Center as Work Unit Number 1-1568-013.

INTRODUCTION

The United States Coast Guard (USCG) requested that the David W. Taylor Naval Ship Research and Development Center (DTNSRDC) prepare a proposal to compare the seakeeping characteristics of two USCG patrol boats.

The two boats differ considerably in both gross size and hull form. Further, their operational area overlap is ill-defined. Hence, DTNSRDC proposed that the comparison be made on a nondimensional basis using computed, regular wave responses. The USCG accepted this proposal, and work was initiated at DTNSRDC. This report documents the results of the DTNSRDC effort.

DATA BASE COMPUTATIONS

Responses to be compared were roll amplitude over maximum wave slope (ϕ_A/ν_H) , pitch amplitude over maximum wave slope (θ_A/ν_H) , heave amplitude over wave amplitude (z_A/ζ_A) , and absolute vertical acceleration in gravity units (\ddot{s}_A/g) . For each boat, these responses were to be computed for all combinations of three Froude numbers (F_n) , 'round the clock relative headings (μ) at

30-degree increments, and at least 10 wavelength to ship length ratios (λ/L). The DTNSRDC Ship Motion and Sea Load Computer Program, reference L^{\pm} , was to be used for the motion computations. Subsequently, acceleration was to be computed using the data obtained from the cited program.

Offsets were read from the lines of the two boats to provide input for the Ship Motion and Sea Load computer program. The resultant hull models are delineated by Figures 1 and 2 and by Table 1. It should be noted that the gross hull dimensions and inertial characteristics presented in Table 1 were input directly, but that the hydrostatic properties given in the same table were computed using the offset data.

The maximum speed of the 95-foot boat corresponds to $F_n=0.63$ while that of the 140-foot boat corresponds to $F_n=0.44$. Hence, in view of the comparative nature of the investigation, it was decided to adopt $F_n=0.44$ as the maximum value for data base computations. The remaining two Froude numbers were arbitrarily specified to be 0.10 and 0.27.

Specification of λ/L values from 0.2 to 2.0 in increments of 0.1 and thence to 3.6 in increments of 0.2 completed preparation of input for the Ship Motion and Sea Load computer program. Computations were subsequently performed for both boats. Preliminary inspection of the results of these computations indicated two problem areas. The iterative procedure used by the program to determine rolling motion did not converge properly for the 14G-foot boat, and very large pitch and heave amplitudes were predicted for both boats in following and near-following waves at the higher Froude numbers.

The rolling motion of the 140-foot boat was recomputed using the technique described in reference 2. No comparable alternative existed for computing pitch and heave, so the amplitudes were accepted as originally computed. It is of interest to note that experiments with radio-controlled models, reference 3, have indicated that broaching-to may occur under conditions similar to those for which the seemingly excessive pitch and heave amplitudes were predicted.

Absolute vertical acceleration at an assigned location includes a pitchinduced component proportional to the distance from the center of pitch (assumed

References are listed on page 6.

to be the LCB) to the assigned location. It was felt that this distance should be made equal for the two boats in order to compare them on a fair basis. Hence, the distance was taken to be that from the LCB to the forward perpendicular of the smaller boat, i.e., 49.7 feet.

Acceleration amplitudes at the specified location ere computed as the second time derivative of the vector sum of heave and pitch components. For these computations it was assumed that θ_{A} in radians was equal to the tangent of θ_{A} , i.e., that θ_{A} was "small." The actual discrepancies between θ_{A} in radians and the tangent of θ_{A} were always less than three percent.

ANALYSIS

For each boat, the computations just described produced over 500 values of each response considered. So, an initial alysis procedure which would isolate critical areas for detailed investigation as needed. To this end, plots comparing the ranges of each response over 1/L at constant speed were constructed as a function of heading. The range minima proved to be of little interest: they were nearly identical for the two boats, and were typically on the order of zero. Range maxima, on the other hand, gave the desired indication of critical areas. So, maxima plots are presented by Figures 3 through 14.

The maxima plotted in each of these figures apply to a λ/L range from 0.2 to 3.6. Heading is defined such that μ = 180 degrees implies head waves, and straight lines are arbitrarily used to connect points at the headings for which computations were made. Response scales are kept constant across speed, and the larger pitch and heave maxima which occurred in following and near-following waves are off-scale. However, the missing points are indicated by arrows; and their numerical values are supplied.

Roll maxima for the two boats, see Figures 3, 4 and 5, differ significantly in magnitude and/or trend at all Froude numbers.

Across heading, the 140-foot boat always exhibits higher maxima than the 95-foot boat. The greatest difference occurs at μ = 90 degrees and F_n = 0.10 (Figure 3) where the roll of the 140-foot boat is more than twice that of the 95-foot boat. Transfer functions for the two boats in the maximum difference

condition are compared in Figure 15. The large difference is not surprising in view of the sectional shapes of the two boats.

With respect to trend differences in roll, it is apparent from Figures 3 through 5 that the 140-foot boat rolls more in beam and quartering regular waves while the 95-foot boat rolls more in bow regular waves. This situation is attributable to the difference between the rolling periods of the two boats. As can be inferred from Figure 15, the 140-foot boat has a much longer roll period than the 95-foot boat. So, bow regular wave encounter frequencies tend to excite the 95-foot boat at roll resonance; but do not attain the relatively low values associated with roll resonance for the 140-foot boat. Figure 16 illustrates this point.

Regions of ill-defined pitch maxima (see Figures 6 through 8) occur at $\mu = 0$ degrees and $\mu = 30$ degrees when $F_n = 0.27$ and $F_n = 0.44$. Elsewhere, the pitch maxima for the two boats exhibit similar trends. Magnitudes are larger for the 140-foot boat, and the discrepancies increase with F_n . The largest discrepancies occur at $F_n = 0.44$ when $\mu = 150$ degrees and when $\mu = 180$ degrees. Then the pitch of the 140-foot boat reaches twice that of the 95-foot boat. Figure 17 compares pitch transfer functions for the $\mu = 180$ degree case.

The tenor of the heave maxima results presented in Figures 9, 10 and 11 is similar to that just described for pitch. However, the largest differences in heave never reach the factor-of-two level associated with roll and pitch. As detailed by Figure 18, the largest differences in heave are on the order of 60 percent.

The acceleration maxima for the two boats, as presented in Figures 12 through 14, exhibit similar trends and do not differ greatly in magnitude. Though the accelerations of the 95-foot boat are marginally higher than those of the 140-foot boat in most conditions, the major differences favor the 95-foot boat. Figure 19 shows acceleration transfer functions for the maximum difference case; here the acceleration of the 140-foot boat exceeds that of the 95-foot boat by about 30 percent.

Two additional notes are in order regarding the acceleration comparisons. First, the high values of pitch and heave which occurred in following and near-following regular waves at the higher Froude numbers were used to compute

accelerations for these conditions. However, the associated encounter frequencies were sufficiently low that the computed accelerations did not obviously reflect the large pitch and/or neave magnitudes. Second, the fact that the accelerations of the 95-foot boat sometimes exceeded those of the 140-foot boat in conditions for which the 140-foot boat experienced larger maximum pitch and heave was due to the more favorable phase relationships of the 140-foot boat. As computed, acceleration is proportional to the cosine of the heave-to-pitch phase angle, $\varepsilon_{z\bar{z}}$. Figure 20 exhibits a plot of the cosine of $\varepsilon_{z\bar{z}}$ for a condition such that the maximum accelerations of the 95-foot boat exceeded that of the 140-foot boat though the maximum pitch and heave of the 140-foot boat exceeded those of the 95-foot boat.

In summary, the most outstanding differences between the two boats occur in beam regular waves at $F_n=0.10$ and in head regular waves at $F_n=0.44$. In the former condition, the roll maximum of the 140-foot boat greatly exceeds that of the 95-foot boat. In the latter condition, the pitch, heave and acceleration maxima of the 140-foot boat significantly exceed those of the 95-foot boat.

CONCLUSION

The preceding analysis indicates that the seakeeping performance of the 95-foot boat is generally superior to that of the 140-foot boat. It should, however, be borne in mind that the analysis was based on nondimensional responses in regular waves. Comparing the dimensional responses of the two boats in identical, random waves could reverse the trend favoring the 95-foot boat if a family of narrow wave spectra with high modal frequencies was selected.

ACKNOWLEDGMENTS

Mr. T. Applebee of DTNSRDC was responsible for the computer applications required to generate the data base; and Mr. R. Watkins, also of DTNSRDC assisted with the data analysis effort.

REFERENCES

- 1. Meyers, W.G. et al., "Manual: NSRDC Ship Motions and Sea Load Computer Program," NSRDC Ship Performance Department Report 3376, February 1975.
- 2. Conolly, J.E., "Roiling and its Stabilization by Active Fins," Quarterly Trans. RINA, Vol. 111, No. 1, pp. 21-48, January 1969.
- 3. Nicholson, K., "Some Parametric Model Experiments to Investigate Broachingto," Paper No. 17, International Symposium on the Dynamics of Marine Vehicles and Structures in Waves, University College, London, April 1974.

THE WAS INTO THE WAS A STATE OF THE WAS INTO THE WAS INTO

TABLE 1 - PROPERTIES OF THE 95-FOOT WPB AND OF THE 140-FOOT WAGB

Parameter	Units	95-foot WPB	140-foot WAGB
LBP	feet	90.0	130.0
B _X	feet	18.4	33.7
T	feet	5.5	11.1
ZG	feet	1.9	2.8
k _e	feet	0.24 L _{BP}	1.24 L _{BP}
k _ф	feet	0.4 B _x	0.4 B _×
Δ	long tons in salt water	102	605
LCB	feet aft of midship	4.70	2.45
KB	feet	3.64	6.78
LCF	feet aft of midship	7.90	1.59
GM	feet	4.63	2.78

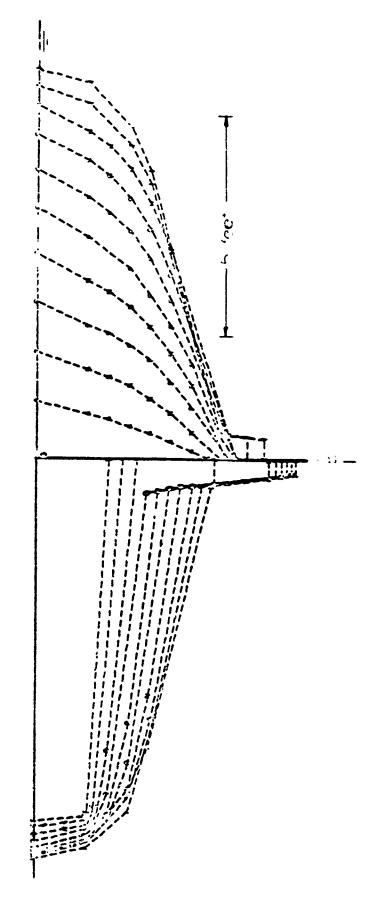


Figure 1 - Computer Representation of 95-foot WPB Hull

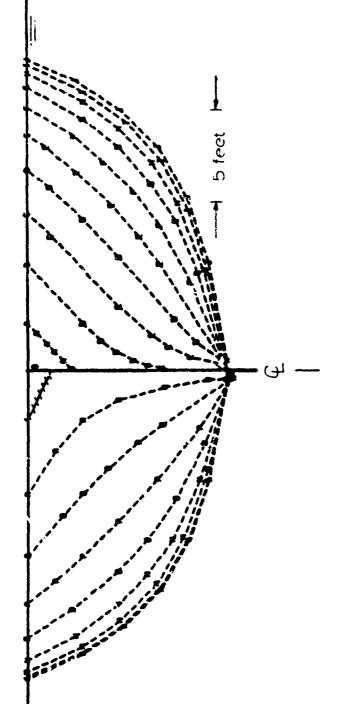


Figure 2 - Computer Respresentation of 146-foot WAGB Hull

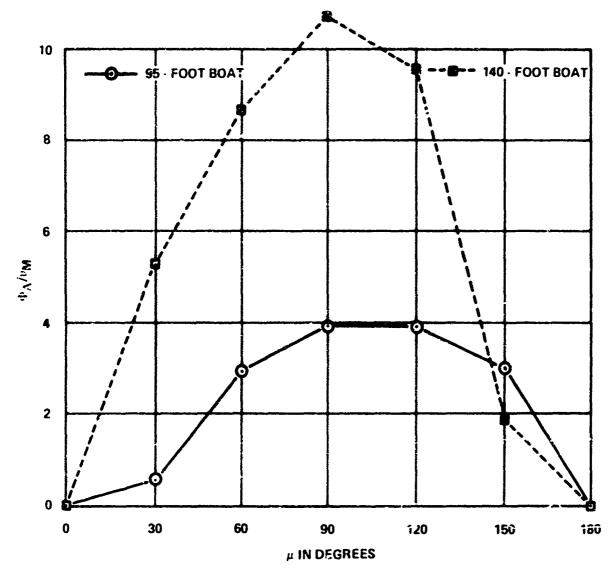


Figure 3 - Roll Maxima at $F_n = 0.10$

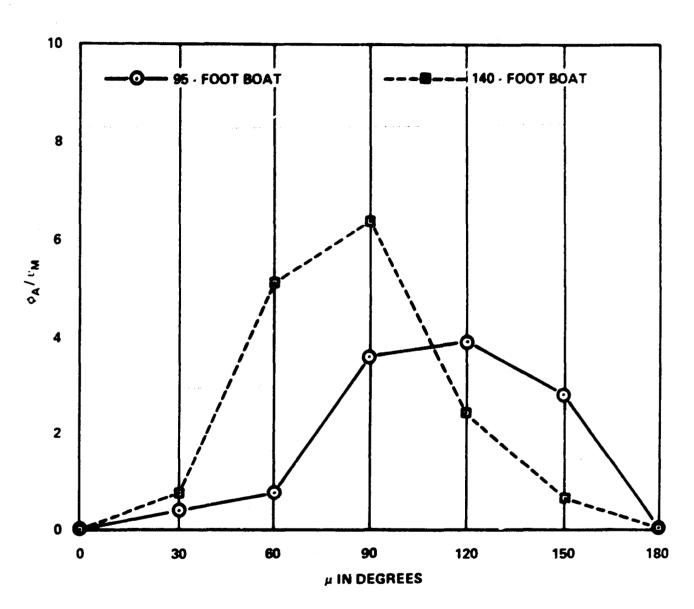


Figure 4 - Roll Maxima at $F_n = 0.27$

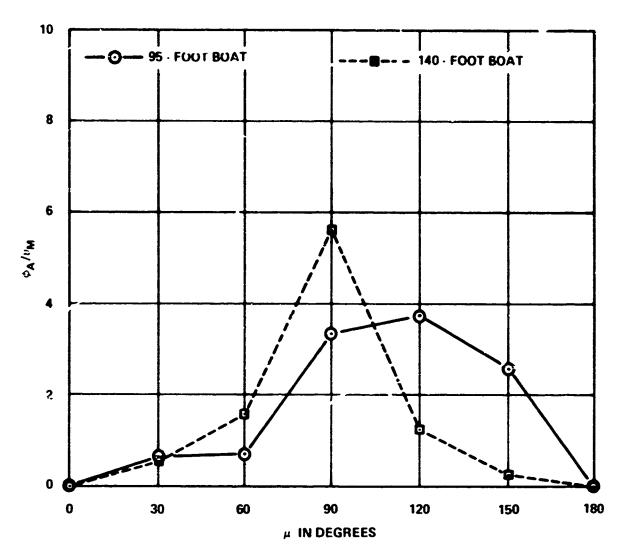


Figure 5 - Roll Maxima at $F_n = 0.44$

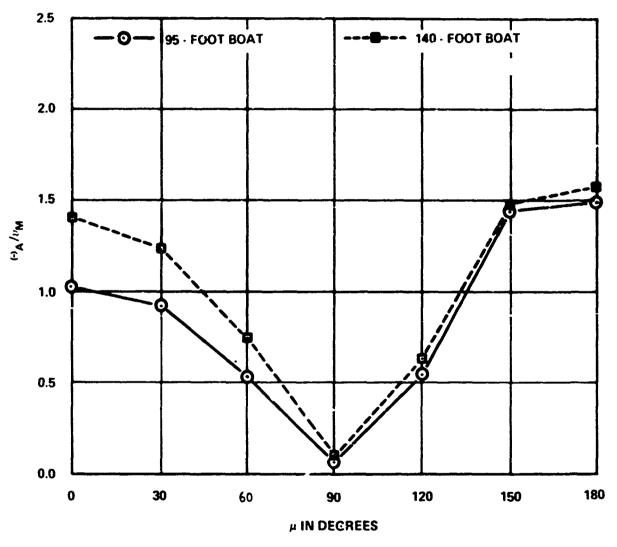


Figure 6 - Pitch Maxima at $F_n = 0.10$

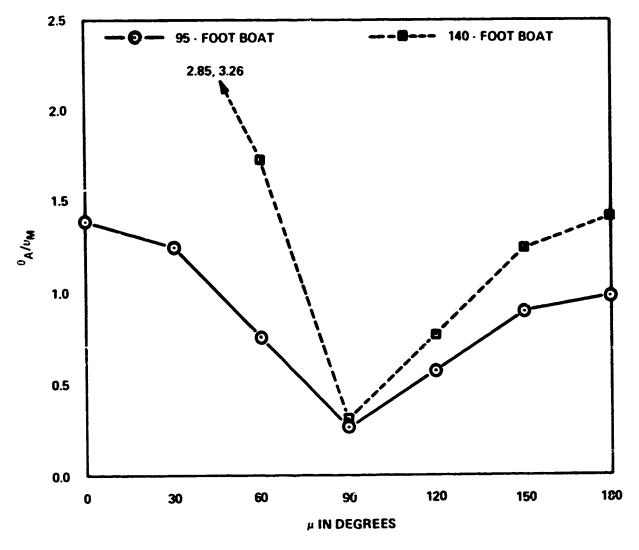


Figure 7 - Pitch Maxima at $F_n = 0.27$

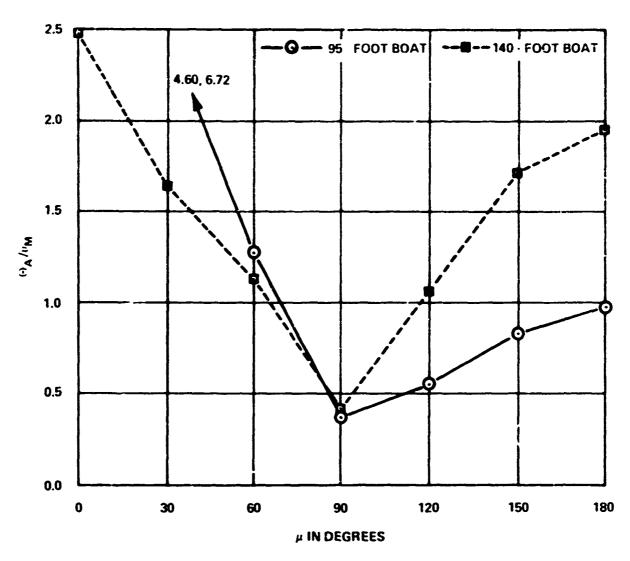


Figure 8 - Pitch Maxima at $F_n = 0.44$

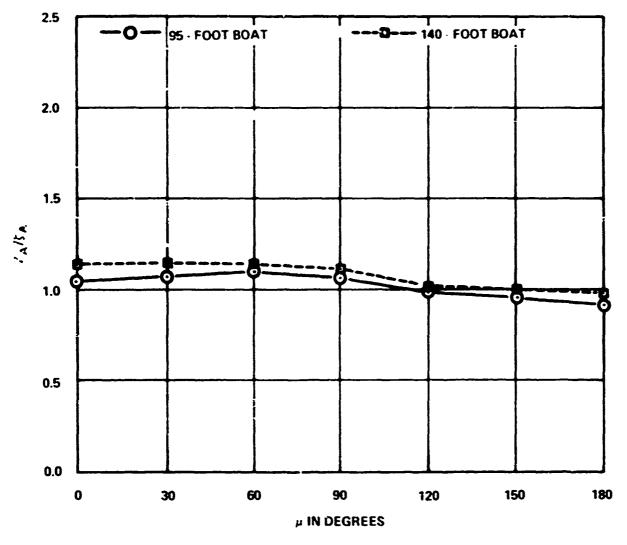


Figure 9 - Heave Maxima at $F_n = 0.10$

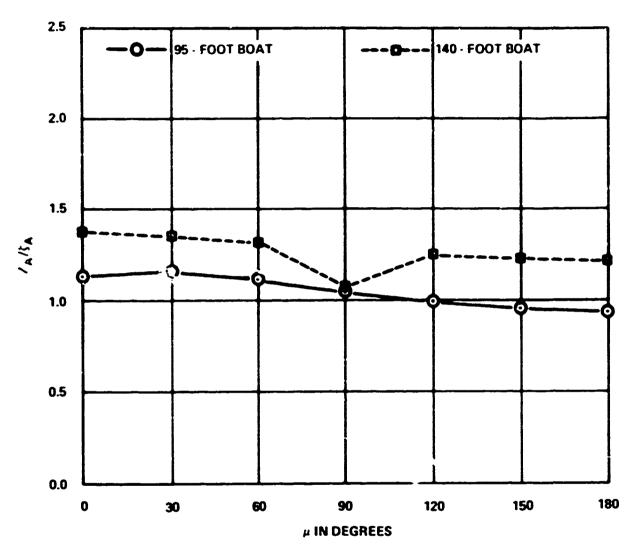


Figure 10 - Heave Maxima at $F_n = 0.27$

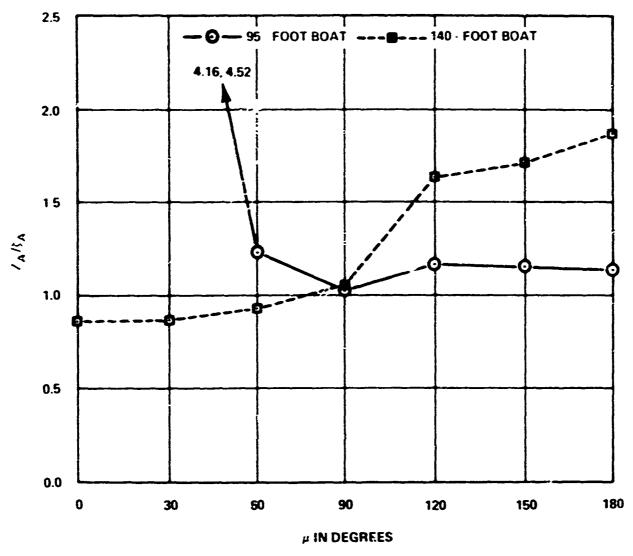


Figure 11 - Heave Maxima at $F_{\rm m}=0.44$

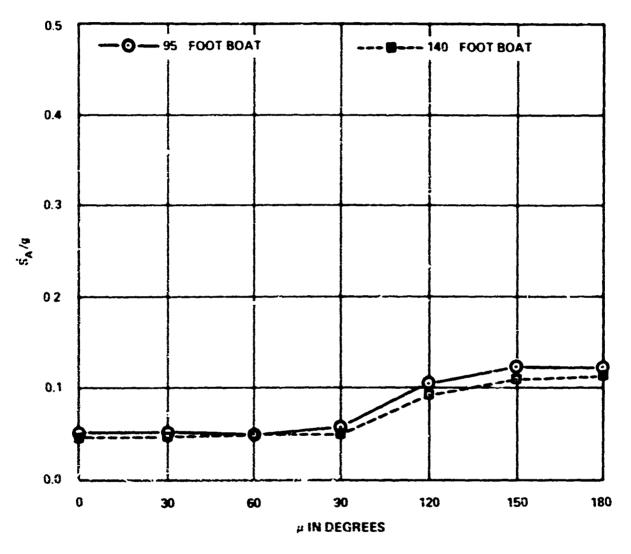


Figure 12 - Acceleration Maxima at $F_p = 0.10$

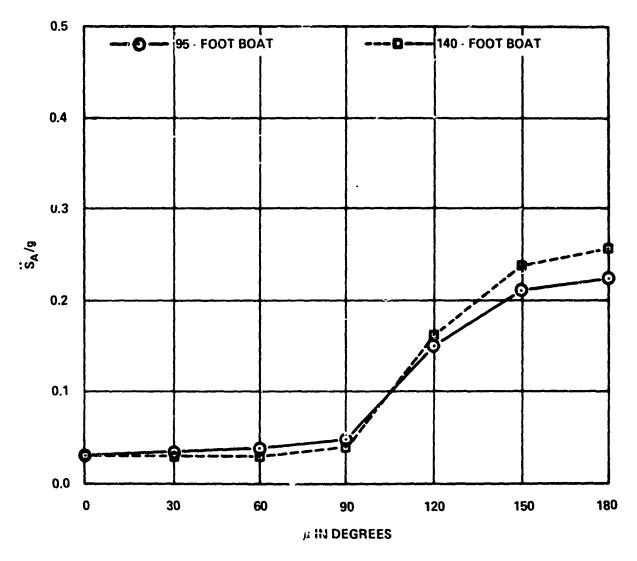


Figure 13 - Acceleration Maxima at $F_n = 0.27$

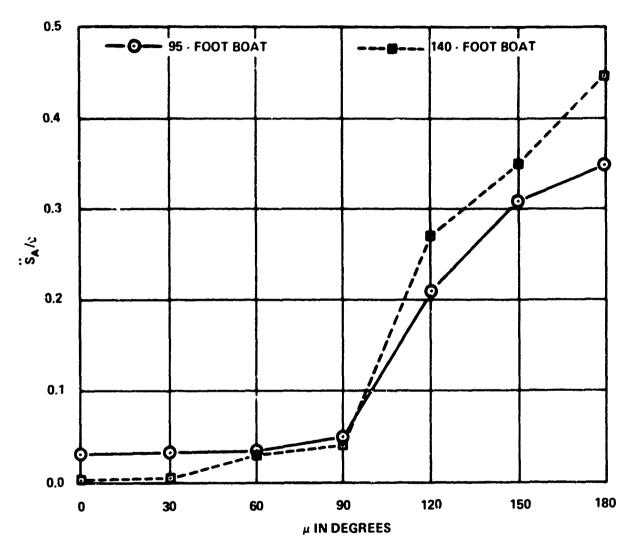


Figure 14 - Acceleration Maxima at $F_n = 0.44$

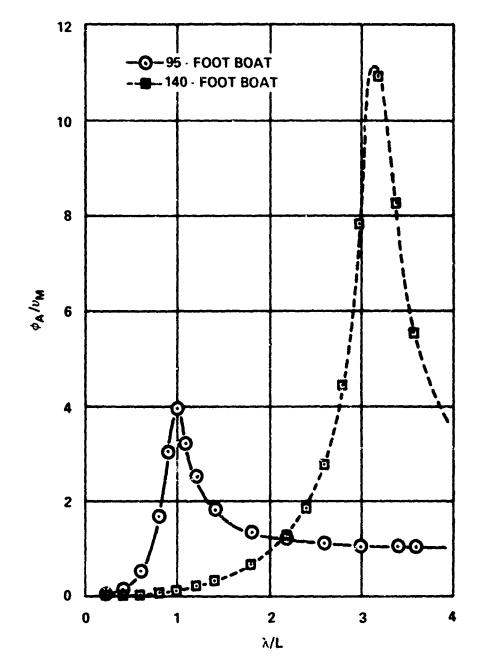


Figure 15 - Roll Transfer Functions at μ = 90 Degrees and F_n = 0.10

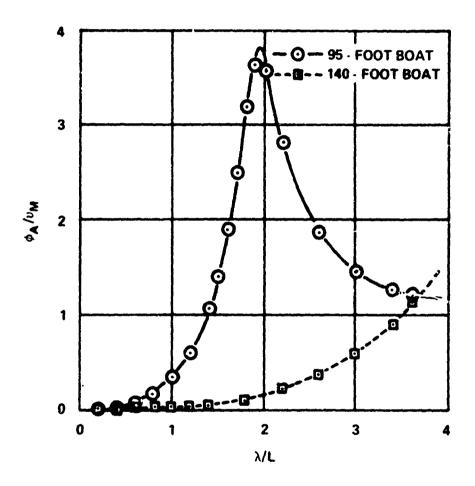


Figure 16 - Roll Transfer Functions at μ = 120 Degrees and $F_{\rm n}$ = 0.44

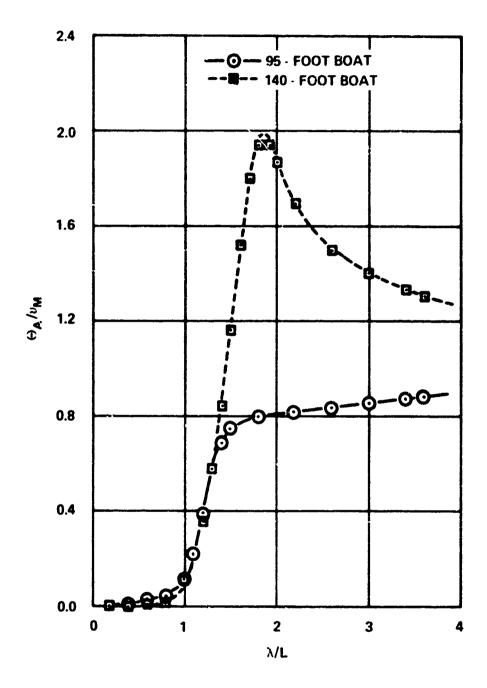


Figure 17 - Pitch Transfer Functions at μ = 180 Degrees and F_{η} = 0.44

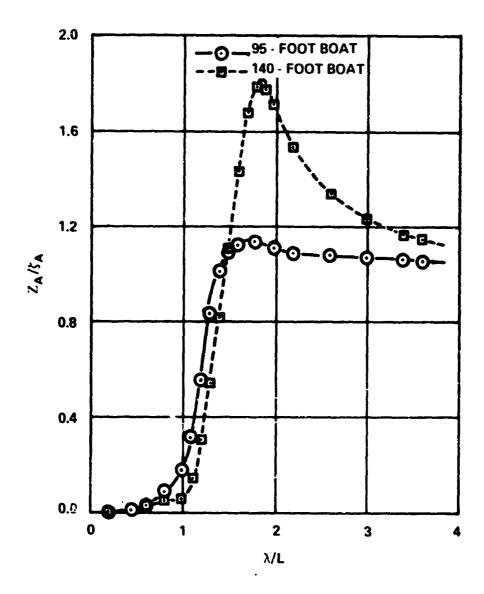


Figure 18 - Heave Transfer Functions at μ = 180 Degrees and F = 0.44

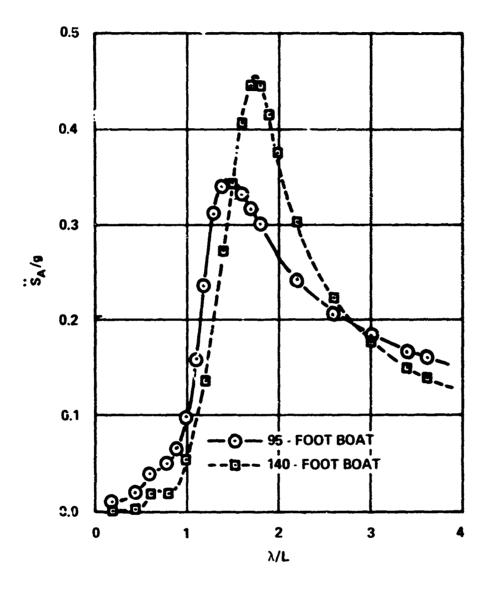


Figure 19 - #:celeration Transfer Functions at μ = 180 Degrees and F = 0.44

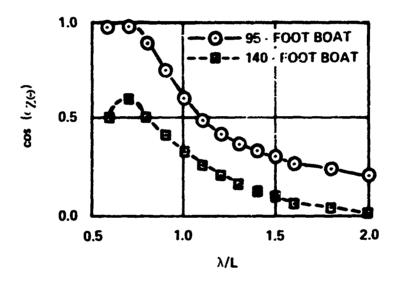


Figure 20 - Cosine of Heave-to-Pitch Phase Angles at μ = 150 Degrees and F = 0.10